Supplementary Materials

Endothelial cell-derived exosomes trigger a positive feedback loop in osteogenesis-angiogenesis coupling via up-regulating zinc finger and BTB domain containing 16 in bone marrow mesenchymal stem cell

Authors:

Lu Liu[1,2,3], Nan Zhou[4], Songning Fu[2], Linlin Wang[5], Yadong Liu[2], Changfeng Fu[2], Feng Xu[2], Weiying Guo[5], Yanhua Wu[6], Jin Cheng[7], Jun Dai[8], Yipeng Wang[9], Xiaofeng Wang[1,*], Qiwei Yang[3,*], Yuanyi Wang[2,*]

Affiliations:

1 Department of Stomatology, China-Japan Union Hospital of Jilin University, Changchun, Jilin, 130033, China.

2 Department of Spine Surgery, The First Hospital of Jilin University, Changchun, Jilin, 130021, China.

3 Medical Research Center, The Second Hospital of Jilin University, Changchun, Jilin, 130041. China.

4 Department of Orthopedics, The First Affiliated Hospital of Zhengzhou University, Henan, 450052, China.

5 Department of Endocrinology, The First Hospital of Jilin University, Changchun, Jilin, 130021, China.

6 Department of Epidemiology, The First Hospital of Jilin University, Changchun, Jilin, 130021, China.

7 Department of Sports Medicine, Peking University Third Hospital, Beijing, 100191, China.

8 Department of Orthopedics, The Second Affiliated Hospital of Soochow University, Jiangsu, 215004, China.

9 Department of Orthopedics, Peking Union Medical College Hospital, Beijing, 100730, China.

*** Corresponding authors:**

Yuanyi Wang: wangyuanyi@jlu.edu.cn

Qiwei Yang: yangqw@jlu.edu.cn

Xiaofeng Wang: wangxiaofeng@jlu.edu.cn

Supplementary Materials

Table S4. The sequence of primers used in this study.

Gene symbol	Forward sequence (5'- 3')	Reverse sequence (5'- 3')
hGAPDH	CGGACCAATACGACCAAATCCG	AGCCACATCGCTCAGACACC
Osterix	CCTCTGCGGGACTCAACAA	CAGGTGAAAGGAGCCCATTAG
OPN	CGCAGACCTGACATCCAGT	GGCTGTCCCAATCAGAAGG
OCN	GTAGTGAAGAGACCCAGGCG	CTCCTGAAAGCCGATGTGGT
CD31	CCCCACTGAAGACGTCGAAT	TCTCCAGACTCCACCACCTTACTT
EMCN	TTTGTACCGAATGTGCT	TTCACGCTCTCTTTATCAGAC
HIF-1α	ACCGCTGAAACGCCAAAG	TCCATCGGAAGGACTAGGTGTCT
ZBTB16	AGAGCACACTCAAGAGCCAC	GCACCCTATAGTGCGTCTCC

Table S5. The antibodies used for western blot in this study.

Antibody	Host	Supplier	Catalog	Dilution
Calnexin	Rabbit	Abcam	ab133615	1:1000
Hsp70	Rabbit	Abcam	ab181606	1:1000
TSG101	Rabbit	Abcam	ab125011	1:1000
CD63	Rabbit	Abcam	ab134045	1:1000
CD81	Rabbit	Abcam	ab109201	1:1000
ZBTB16	Rabbit	Abcam	ab305064	1:1000
CD31	Rabbit	Bioss	bs-0468R	1:1000
EMCN	Rat	Abcam	ab106100	1:1000
HIF-1α	Rabbit	Proteintech	20960-1-AP	1:1000
β-actin	Rabbit	Servicebio	ZB15001-HRP-100	1:2000

Table S6. The antibodies used for IF stain in this study.

Antibody	Host	Supplier	Catalog	Dilution
ZBTB16	Mouse	Santa Cruz Biotechnology	sc-28319	1:50
Osterix	Mouse	Santa Cruz Biotechnology	sc-393325	1:50
CD31	Mouse	Invitrogen	48-0319-42	1:100
EMCN	Rat	Invitrogen	50-5851-82	1:100

Supplementary Results

Confirm the co-culture system

For the ratio of hBMSCs and HUVECs in co-culture system, we explored the proliferation, angiogenesis, and osteogenic abilities of cells in a series of gradient ratios. The results showed that BMSCs and HUVECs had the best proliferation, angiogenesis, and osteogenic abilities in a 1:1 ratio, which indicates that this is the most optimal coupling effect between them (Fig. S1). Therefore, a 1:1 ratio was used for the co-culture system in subsequent experiments.

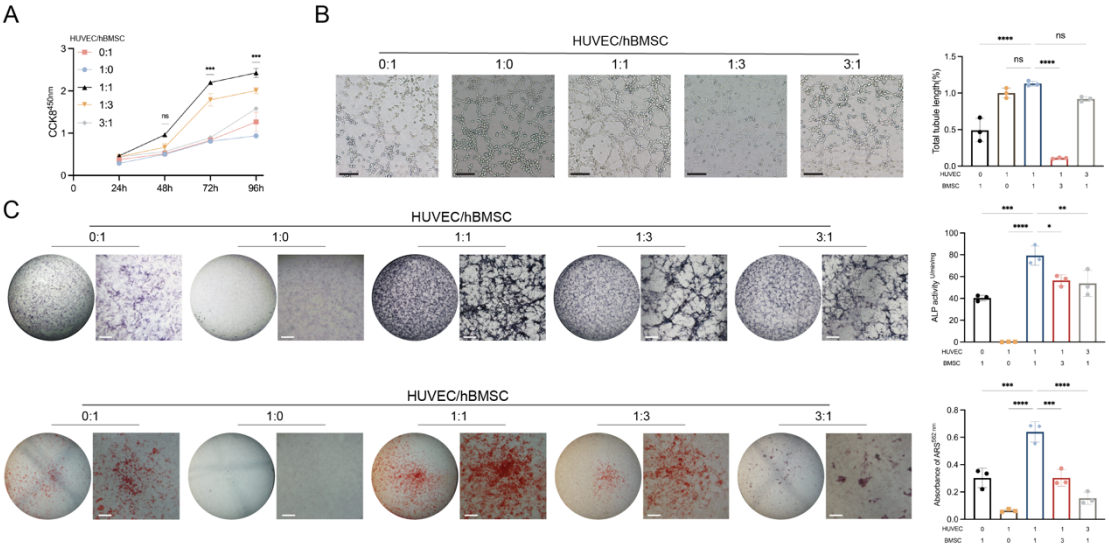

Fig. S1 hBMSCs and HUVECs co-cultured in different ratios.

The impact of GW4869 on BMSC differentiation

Fig. S2 showed that GW4869 partially inhibited the osteogenic differentiation of BMSCs, possibly due to the inhibition of endogenous exosome secretion. However, when comparing BMSCs with or without GW4869 treatment and co-culture systems with or without GW4869 treatment, this difference was overwhelmed by the differences between the two co-culture systems. This indicates that GW4869 has a more significant impact on the osteogenic process during the coupling of two types of cells, rather than solely inhibiting the osteogenic differentiation of BMSCs.

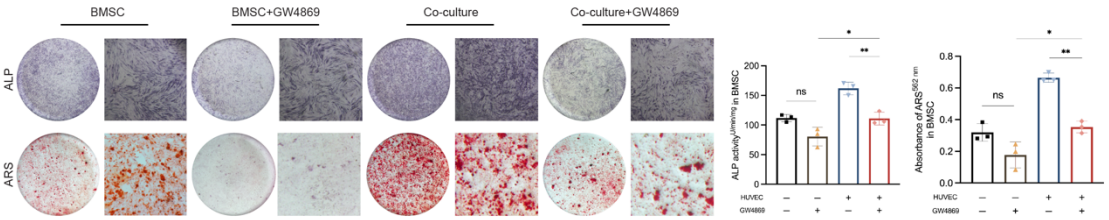

Fig. S2 The impact of GW4869 on BMSC differentiation

Enrichment analysis of RNA-seq results

The enrichment analysis of RNA-seq results including GO analysis (Fig. S3A), KEGG pathway (Fig. S3B), and the heatmap of the clustered differentially expressed genes (Fig. S3C) in hBMSCs after EC-exo treatment were showen in Fig. S3. The principal components analysis (PCA) results showed that the EC-exo treatment group emerged more significant transcriptome changes on the distribution of principal component 2 (Fig. S3D).

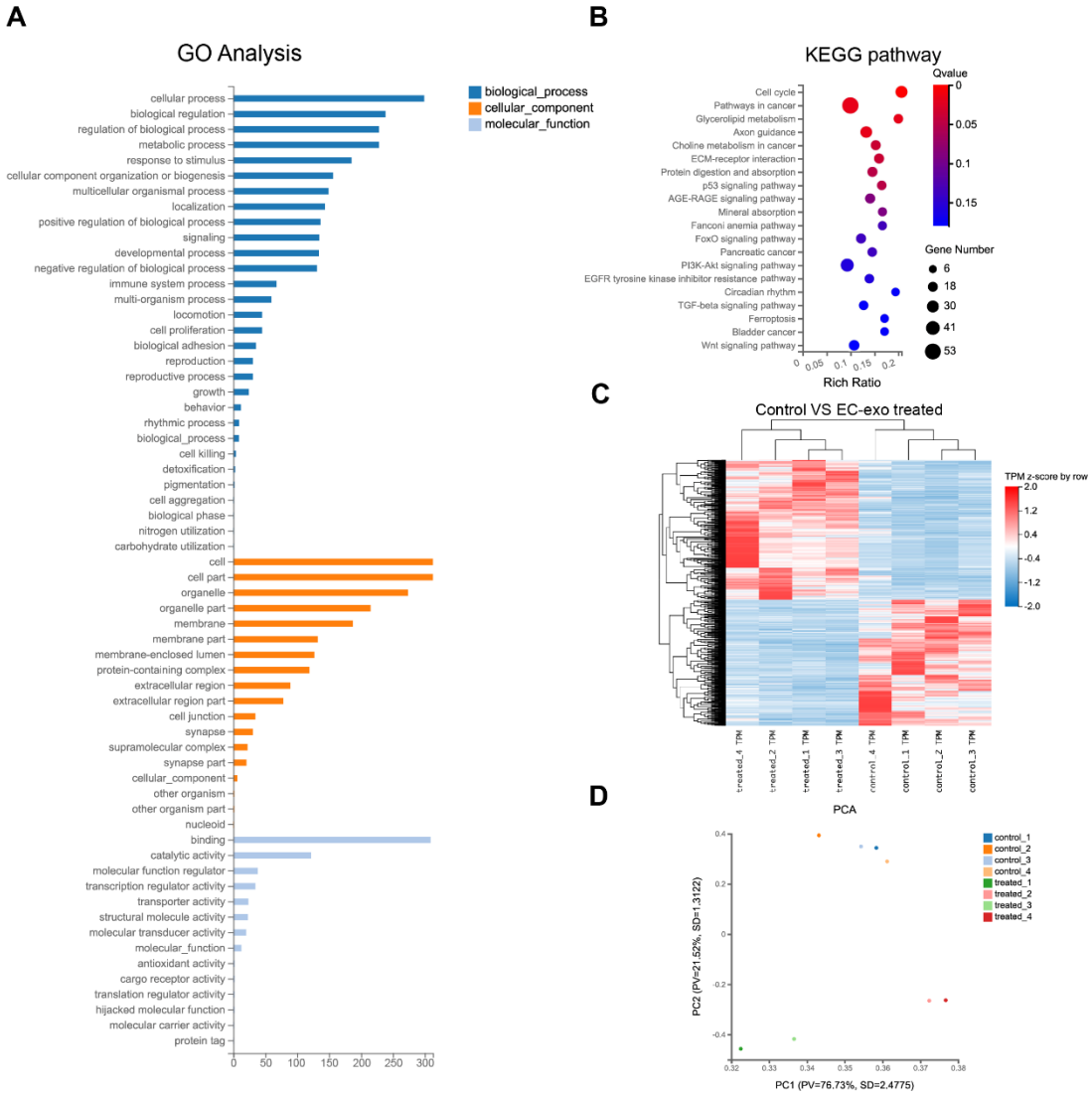

Fig. S3 Enrichment analysis of RNA-seq results

The impact of knockout ZBTB16 on hBMSCs

We knockout ZBTB16 in hBMSCs and detected their proliferation, cell viability/cytotoxicity, and osteogenic differentiation abilities. The results showed that after ZBTB16 knockout, the proliferation ability (Fig S4A) and activity (Fig S4B) of hBMSCs was not affected, while their osteogenic differentiation ability was significantly weakened (Fig S4C).

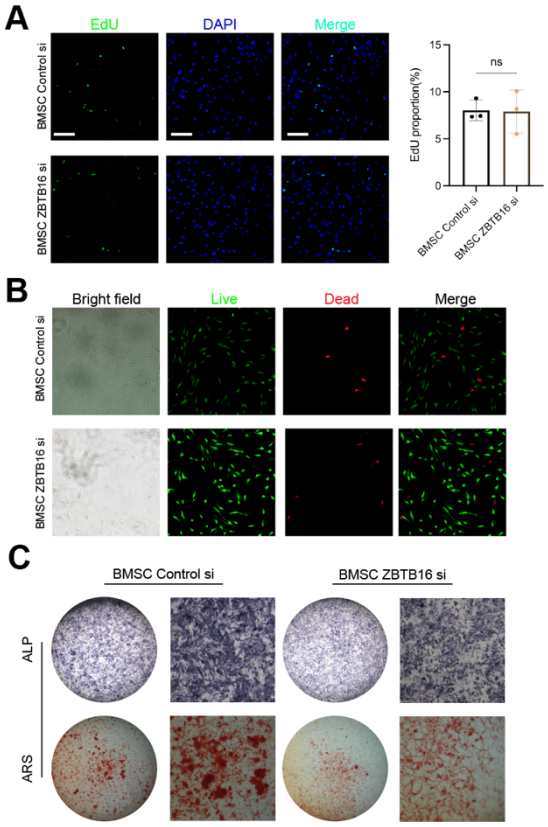

Fig. S4 The impact of knockout ZBTB16 on hBMSCs

Biosafety assessment of EC-exo

After 3 weeks of EC-exo treatment, we dissected and extracted major organs (heart, liver, spleen, lung, and kidney) from rats. H&E staining showed that EC-exo did not cause pathological changes in these tissues (Fig. S5). Scale bar represents 100 μm.

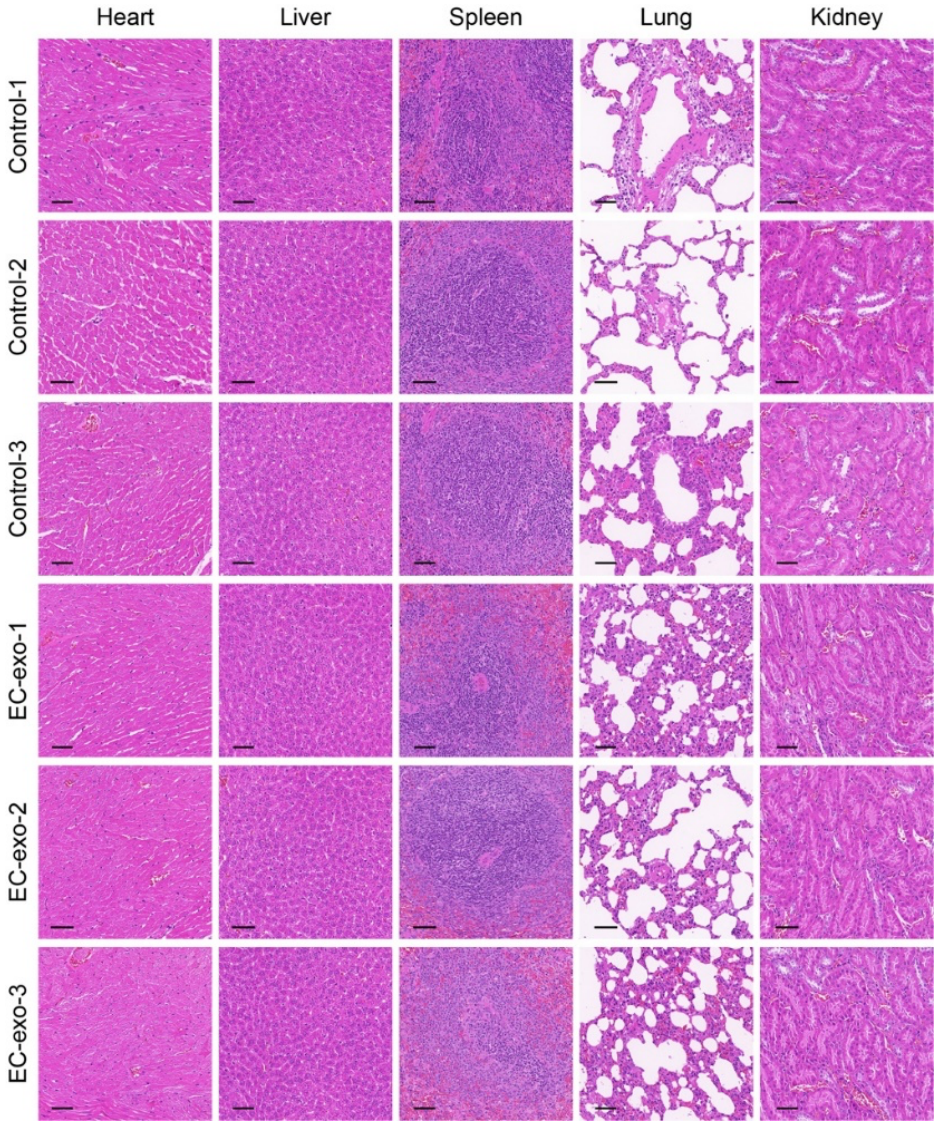

Fig. S5 H&E staining images of major organs after EC-exo treatment

Identification of hBMSCs

The hBMSCs were identified by flow cytometry to exhibit typical features of MSCs, namely negative hematopoietic stem cell markers (CD34 and CD45) and positive MSC markers (CD73 and CD90) (Fig. S6). The results of flow cytometry support that the extracted cells are BMSCs.

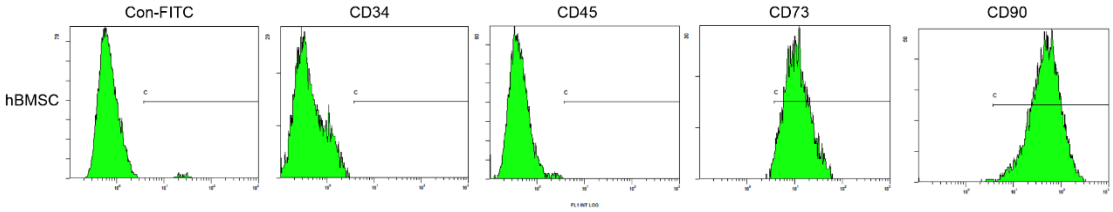

Fig. S6 Flow cytometry detection of extracted hBMSCs.

Residency of EC-exo at the site of injury

In order to ensure the sustained concentration of EC-exo at the site of injury, we tracked the local retention of EC-exo after injection during the pilot phase. Specifically, we stained EC-exo with DiR and injected 50μg of EC-exo into the injured site of the tibial defect SD rat models. On the 1st, 3rd, and 5th day after injection, the residual EC-exo at the site of injury was detected through live animal imaging. The results showed that on the first day after injection of EC-exo, the fluorescence range was relatively limited. On the third day, EC-exo further diffused and maintained local high concentrations. On the fifth day, the concentration slightly decreased. The results are shown in the newly added Figure S7. In view of this, we chose to administer EC-exo every 3 days to maintain its sustained retention at the site of injury and maximize its therapeutic effect (Fig. S7).

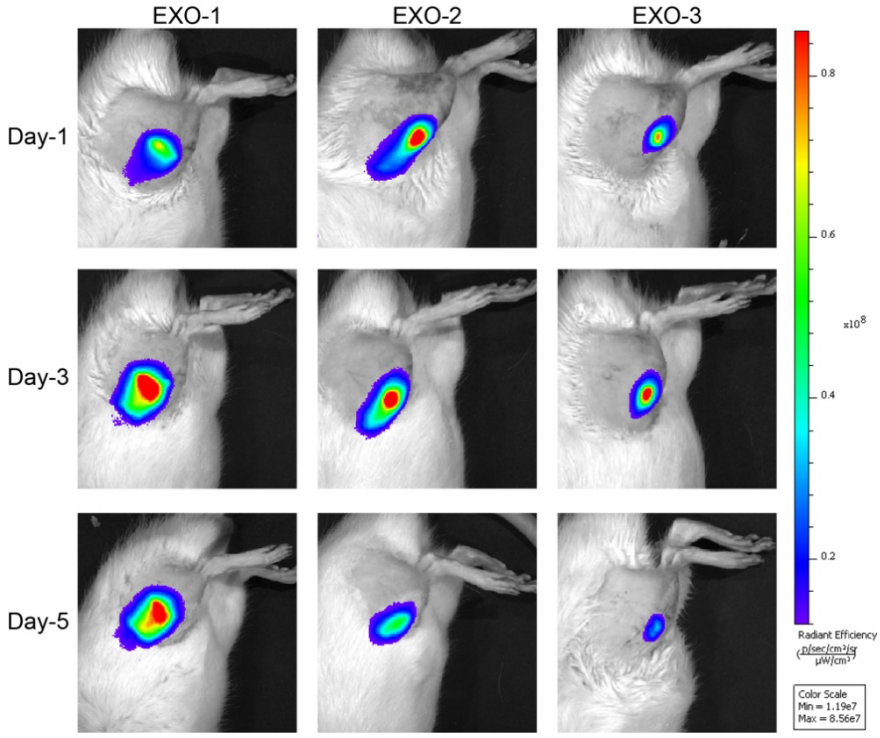

Fig. S7 Residency of EC-exo at the site of injury